arXiv:1408.3722v1 [cond-mat.soft] 16 Aug 2014

A tensor model for nematic phases of bent-core molecules based on molecular theory

Jie Xu[1] & Pingwen Zhang[1*]

[1]LMAM & School of Mathematical Sciences, Peking University, Beijing 100871, China

E-mail: rxj_2004@126.com, pzhang@pku.edu.cn

August 19, 2014

Abstract

A tensor model for nematic phases of bent-core molecules is presented. The model is derived from the second virial expansion. The terms in the model are determined by the C_{2v} symmetry of the molecule, and the coefficients are estimated from molecular parameters. An extension of the Bingham closure is employed that is able to restrict the tensors in physical range. The model can describe the homogeneous uniaxial and biaxial nematics, as well as the twist-bend and the splay-bend modulation. Two new modulated phases are found. Some of the phase sequences we obtain have been observed experimentally.

1 Introduction

The study of bent-core molecules has become a very attractive area in the research of liquid crystals. Numerous kinds of bent-core molecules with various molecular structures have been synthesized, which exhibit diverse phase behaviours. They also show rich responses to external fields, thus are expected to have practical applications. A bent-core molecule is of C_{2v} symmetry that differs from $D_{\infty h}$ symmetry of a rod-like molecule, which leads to more complex orientational order. The polar and biaxial local order, as well as the spatial variation of orientation, is notable in many modulated phases, no matter in layer or columnar structures [1, 2]. This is not common in equilibrium phases of rod-like molecules. Even if the concentration is constant in space, it is still possible to exhibit nematic modulated phases that purely alter in orientation. The possibilities of these phases have been predicted earlier [3], and lately the twist-bend phase, one of the predictions, has been identified experimentally [4, 5]. To have a clear understanding of these behaviours, the modeling of orientation variation is crucial.

In contrast to a huge number of experiments, only a few theoretical models are proposed for inhomogeneous phases of bent-core molecules. Lorman and Mettout [6] examined the antiferroelectric polarization of nematic phases. Roya and Madhusudana [7] considered the interplay of polarization and density fluctuation to model transitions between layer and columnar structures. Roy *et al.* [8] focused on the layer structures, and Vautopič *et al.* [9] studied tilt layer structures. Shamid *et al.* [10] proposed a modification of Oseen-Frank energy to model the twist-bend phase and the splay-bend phase, and recently a model more generic is examined by Vaupotič *et al.* [11]. The twist-bend phase is also discussed by Virga [12]. There are also some tensor models for homogeneous phases other than the uniaxial nematic phase [13, 14]. These models are helpful to understanding the phase behaviours. However, they are established based on the comprehension of the phases and are only able to examine specific phase transitions. At the same time, these phenomenological models focus on the phase transitions themselves, regardless of the species of molecules that would exhibit these phase transitions.

*Corresponding author

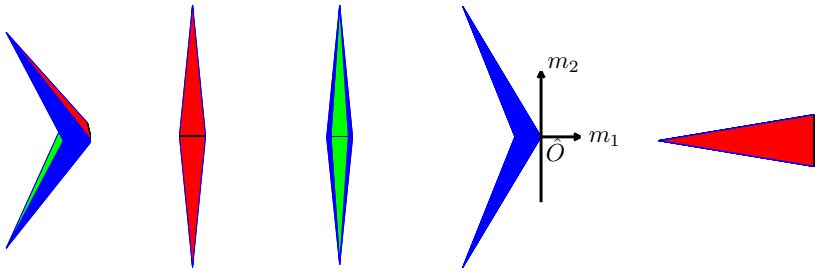

Figure 1: Representation of a bent-core molecule. The front of the molecule is colored red, the back is colored green, and the sides are colored blue. From left to right: oblique view, front view, back view, side view, top view.

It is desirable to construct a unified model for bent-core molecules in which the molecular parameters are built and all the possible phase transitions can be covered. In this paper, we derive the following model from molecular theory.

$$\begin{aligned}\frac{F[Q_1,Q_2,\boldsymbol{p}]}{k_BT} = \frac{1}{V}\int \mathrm{d}\boldsymbol{x}\Big\{ & c(\boldsymbol{b}\cdot\boldsymbol{p} + B_1 : Q_1 + B_2 : Q_2 - \log Z) \\ & \frac{c^2}{2}(c_{01}|\boldsymbol{p}|^2 + c_{02}|Q_1|^2 + c_{03}|Q_2|^2 + 2c_{04}Q_1 : Q_2) \\ & + c^2(c_{11}p_j\partial_i Q_{1ij} + c_{12}p_j\partial_i Q_{2ij}) \\ & + \frac{c^2}{4}\left[c_{21}|\nabla\boldsymbol{p}|^2 + c_{22}|\nabla Q_1|^2 + c_{23}|\nabla Q_2|^2 + 2c_{24}\partial_i Q_{1jk}\partial_i Q_{2jk}\right. \\ & + 2c_{27}\partial_i p_i\partial_j p_j + 2c_{28}\partial_i Q_{1ik}\partial_j Q_{1jk} \\ & \left. + 2c_{29}\partial_i Q_{2ik}\partial_j Q_{2jk} + 4c_{2,10}\partial_i Q_{1ik}\partial_j Q_{2jk}\right]\Big\}, \end{aligned} \tag{1.1}$$

where k_B is the Boltzmann constant, T is the absolute temperature, V is the volume of the system, and c is the concentration that is constant in space. The body-fixed orthonormal frame $(\hat{O};\boldsymbol{m}_1,\boldsymbol{m}_2,\boldsymbol{m}_3)$, drawn in Fig.1, is posed such that $\hat{O}$ locates at the arrowhead, $\boldsymbol{m}_1$ is along the direction of arrow, and $\boldsymbol{m}_2$ coincides with the direction of string.

$$\begin{aligned}\boldsymbol{p} &= \langle \boldsymbol{m}_1 \rangle, \\ Q_1 &= \langle \boldsymbol{m}_1\boldsymbol{m}_1 \rangle, \\ Q_2 &= \langle \boldsymbol{m}_2\boldsymbol{m}_2 \rangle\end{aligned}$$

are angular moments under the density function

$$\rho = \frac{1}{Z}\exp(\boldsymbol{b}\cdot\boldsymbol{m}_1 + B_1 : \boldsymbol{m}_1\boldsymbol{m}_1 + B_2 : \boldsymbol{m}_2\boldsymbol{m}_2), \tag{1.2}$$

with

$$Z = \int_{SO_3} \mathrm{d}\nu \exp(\boldsymbol{b}\cdot\boldsymbol{m}_1 + B_1 : \boldsymbol{m}_1\boldsymbol{m}_1 + B_2 : \boldsymbol{m}_2\boldsymbol{m}_2),$$

where $\mathrm{d}\nu$ represents the uniform probability measure on SO_3. Here Q_1 and Q_2 are symmetric matrices, and we require that they share an eigenframe and that $\boldsymbol{p}$ is one of the eigenvectors. Accordingly, the same constraint is required for B_1, B_2 and $\boldsymbol{b}$.

This model is based on the virial expansion characterized by intermolecular interaction. The terms in the top two lines of (1.1) constitute the bulk energy, and the rest terms compose the elastic energy. The choice of tensors and the construction of the bulk energy are discussed in [15] and are adopted

here. The terms in the first line are obtained from the entropy term by employing an extension of the Bingham closure, which is able to confine the tensors to physical constraints. Analogous to what is pointed out in [15], the form of elastic energy is determined by the molecular symmetry, and the coefficients are estimated from molecular parameters. As we focus on the nematic phases of bent-core molecules, we assume that the concentration is constant. By removing this assumption and including more terms in the truncation, the modeling procedure can be extended to smectic and columnar phases, which is done for smectic rod-like crystals [16, 17]. The procedure can also be followed in the modeling of generic rigid molecules.

The modeling procedure is based purely on molecular information, carried out in rigorous mathematics, and requires no prior knowledge on the phase structures. In [16] a similar approach is done for rod-like molecules, which connects several classical models for rod-like molecules. In addition, we do not see any tensor model that includes spatial inhomogeneity, while the tensor models for rod-like liquid crystals, first proposed by de Gennes [18] and extended in various forms afterwards, have proved their success in the study of non-bulk effects [19, 20]. Therefore our model is expected to be suitable for all possible phase transitions, as well as phase inhomogeneity, such as interfaces and defects. We will show that our model is able to capture the twist-bend phase and the splay-bend phase, along with two new phases. We also obtain the isotropic — uniaxial nematic — twist-bend and the isotropic — twist-bend sequences. The first sequence has been identified experimentally [4, 5].

The rest of the paper is organized as follows. In Section 2 we illustrate the modeling procedure, deduce the form of the free energy and describe the way of deriving coefficients from molecular parameters. Some numerical results are presented in Section 3. They are compared with previous works. In Section 4, we draw a conclusion and propose some future works. Some proofs and calculations are given in Appendix.

2 The derivation of the tensor model

2.1 The molecular theory

We use $\boldsymbol{x}$ to represent the location of $\hat{O}$ in the space. The orientation of the body-fixed orthonormal frame $(\hat{O}; \boldsymbol{m}_i)$ with respect to the space-fixed orthonormal frame $(O; \boldsymbol{e}_i)$ is denoted by $P \in SO_3$.

$$(\boldsymbol{m}_1, \boldsymbol{m}_2, \boldsymbol{m}_3) = (\boldsymbol{e}_1, \boldsymbol{e}_2, \boldsymbol{e}_3)P.$$

The jth element of $\boldsymbol{m}_i$, denoted by m_{ij}, is located at jth row, ith column in P. If necessary, we will use the notation $\boldsymbol{m}_i(P)$ to express the $\boldsymbol{m}_i$ determined by a certain P. An element in SO_3 can be represented by the Euler angles (α, β, γ).

$$P(\alpha,\beta,\gamma) = \begin{pmatrix} \cos\alpha & -\sin\alpha\cos\gamma & \sin\alpha\sin\gamma \\ \sin\alpha\cos\beta & \cos\alpha\cos\beta\cos\gamma - \sin\beta\sin\gamma & -\cos\alpha\cos\beta\sin\gamma - \sin\beta\cos\gamma \\ \sin\alpha\sin\beta & \cos\alpha\sin\beta\cos\gamma + \cos\beta\sin\gamma & -\cos\alpha\sin\beta\sin\gamma + \cos\beta\cos\gamma \end{pmatrix}. \tag{2.1}$$

The uniform unit measure on SO_3 is denoted by $\mathrm{d}\nu = \frac{\sin\alpha}{8\pi^2}\mathrm{d}\alpha\mathrm{d}\beta\mathrm{d}\gamma$.

We start from the second virial expansion.

$$\begin{aligned} F[f] = F_0 + \frac{k_B T}{V}\Bigg[& \int \mathrm{d}\nu\mathrm{d}\boldsymbol{x} f(\boldsymbol{x}, P)\log f(\boldsymbol{x}, P) \\ & + \frac{1}{2}\int \mathrm{d}\nu(P)\mathrm{d}\boldsymbol{x}\mathrm{d}\nu(P')\mathrm{d}\boldsymbol{x'} f(\boldsymbol{x}, P)G(\boldsymbol{r}, P, P')f(\boldsymbol{x'}, P')\Bigg], \end{aligned} \tag{2.2}$$

where $\boldsymbol{r} = \boldsymbol{x'} - \boldsymbol{x}$, and f is consistent with the total concentration.

$$\frac{1}{V}\int \mathrm{d}\boldsymbol{x}\mathrm{d}\nu f(\boldsymbol{x}, P) = c_0.$$

The kernel function $G(\boldsymbol{r}, P, P')$ is related to the pairwise interaction $U(\boldsymbol{r}, P, P')$ by

$$G(\boldsymbol{r}, P, P') = 1 - \exp(-U(\boldsymbol{r}, P, P')/k_B T). \tag{2.3}$$

The additive constant F_0 is set to zero in the following. Expanding $f(\boldsymbol{x'}, P') = f(\boldsymbol{x} + \boldsymbol{r}, P')$ with respect to $\boldsymbol{r}$, we have

$$f(\boldsymbol{x'}, P') = f(\boldsymbol{x}, P') + \nabla f(\boldsymbol{x}, P') \cdot \boldsymbol{r} + \frac{1}{2}\nabla^2 f(\boldsymbol{x}, P') : \boldsymbol{r}\boldsymbol{r} + \cdots . \tag{2.4}$$

Define

$$M^{(k)}(P, P') = \int G(\boldsymbol{r}, P, P') \underbrace{\boldsymbol{r} \ldots \boldsymbol{r}}_{k \text{ times}} \mathrm{d}\boldsymbol{r}. \tag{2.5}$$

Taking (2.4) into (2.2), we get

$$\begin{aligned} F[f] =& \frac{k_B T}{V} \left[\int \mathrm{d}\nu \mathrm{d}\boldsymbol{x} f(\boldsymbol{x}, P) \log f(\boldsymbol{x}, P) + \frac{1}{2} \int \mathrm{d}\boldsymbol{x} \mathrm{d}\nu(P) \mathrm{d}\nu(P') f(\boldsymbol{x}, P) M^{(0)}(P, P') f(\boldsymbol{x}, P') \right. \\ &+ \frac{1}{2} \int \mathrm{d}\boldsymbol{x} \mathrm{d}\nu(P) \mathrm{d}\nu(P') f(\boldsymbol{x}, P) M^{(1)}(P, P') \nabla f(\boldsymbol{x}, P') \\ &\left. + \frac{1}{4} \int \mathrm{d}\boldsymbol{x} \mathrm{d}\nu(P) \mathrm{d}\nu(P') f(\boldsymbol{x}, P) M^{(2)}(P, P') \nabla^2 f(\boldsymbol{x}, P') + \cdots \right]. \end{aligned} \tag{2.6}$$

The first line is the bulk energy, denoted by F_{bulk}; the second line is about first derivatives of f, thus is called the first-order elastic energy, denoted by $F^{(1)}_{elastic}$; the third line is the second-order elastic energy, denoted by $F^{(2)}_{elastic}$, and so on.

To derive a tensor model, we need to express the bulk and elastic energy in terms of angular moments of f,

$$\langle \boldsymbol{m}_{i_1} \ldots \boldsymbol{m}_{i_k} \rangle .$$

For rod-like molecules, both the terms and the coefficients can be obtained analytically [16] by taking U as the hardcore potential,

$$U(\boldsymbol{r}, P, P') = \begin{cases} +\infty, & \text{if two molecules touch,} \\ 0, & \text{elsewhere.} \end{cases}$$

Unfortunately, this is difficult for bent-core molecules. Therefore, we will follow the route in [15] to find out the form first, which is dependent only on the molecular symmetry.

2.2 The bulk energy

In [15] we have already discussed the representation of $M^{(0)}$. We have proved that $M^{(0)}$ is a function of $\bar{P} = (p_{ij})_{3\times 3} = P^{-1}P'$. The analysis of molecular symmetry gives that to approximate $M^{(0)}$ with a quadratic polynomial of p_{ij}, it reads

$$M^{(0)} = c_{00} + c_{01}p_{11} + c_{02}p_{11}^2 + c_{03}p_{22}^2 + c_{04}(p_{12}^2 + p_{21}^2); \tag{2.7}$$

and a cubic approximation reads

$$\begin{aligned} M^{(0)} =& c_{00} + c_{01}p_{11} + c_{02}p_{11}^2 + c_{03}p_{22}^2 + c_{04}(p_{12}^2 + p_{21}^2) \\ &+ c_{05}p_{11}^3 + c_{06}p_{11}p_{22}^2 + c_{07}p_{11}(p_{12}^2 + p_{21}^2) + c_{08}p_{12}p_{21}p_{22}. \end{aligned} \tag{2.8}$$

Here we adopt (2.7). This choice is not only for simplicity. In Section 3.1 we will show that the inclusion of third-order terms does not affect the phase diagram for homogeneous phases under the

coefficients derived from molecular parameters using the method described in Section 2.4. Denote

$$\begin{aligned}\boldsymbol{p} &= \langle \boldsymbol{m}_1 \rangle \,, \\ Q_1 &= \langle \boldsymbol{m}_1 \boldsymbol{m}_1 \rangle \,, \\ Q_2 &= \langle \boldsymbol{m}_2 \boldsymbol{m}_2 \rangle \,,\end{aligned}$$

where $\langle \cdot \rangle$ is the average of a function under the orientational density function $\rho(\boldsymbol{x}, P) = f(\boldsymbol{x}, P)/c(\boldsymbol{x})$ at $\boldsymbol{x}$. Here $c(\boldsymbol{x}) = \int \mathrm{d}\nu f(\boldsymbol{x}, P)$. The bulk energy is now written as

$$\frac{F_{bulk}}{k_B T} = \frac{1}{V} \int \mathrm{d}\boldsymbol{x} f \log f + \frac{1}{2} \left(c_{00} c^2 + c_{01} |c\boldsymbol{p}|^2 + c_{02} |cQ_1|^2 + c_{03} |cQ_2|^2 + 2c_{04} cQ_1 : cQ_2 \right) .$$

Next we need to express the entropy term as a function of tensors. The entropy term can be written as

$$\int \mathrm{d}\boldsymbol{x} \mathrm{d}\nu f \log f = \int \mathrm{d}\boldsymbol{x} c(\boldsymbol{x}) (\log c(\boldsymbol{x}) + \int \mathrm{d}\nu \rho(\boldsymbol{x}, P) \log \rho(\boldsymbol{x}, P)).$$

Here we are seeking for an extension of the Bingham closure for a single tensor Q. The Bingham closure is obtained by minimizing the entropy term with Q given.

$$\begin{aligned} & \inf \int_{S^2} \mathrm{d}\boldsymbol{m} \rho(\boldsymbol{m}) \log \rho(\boldsymbol{m}), \\ \text{s.t.} \quad & \int \mathrm{d}\nu \rho(\boldsymbol{m}) = 1, \\ & \int \mathrm{d}\nu \boldsymbol{m}\boldsymbol{m} \rho(\boldsymbol{m}) = Q. \end{aligned}$$

By the Euler-Lagrange equation,

$$\rho(\boldsymbol{m}) = \frac{1}{Z} \exp(B : \boldsymbol{m}\boldsymbol{m}), \tag{2.9}$$

where B is a symmetric matrix and

$$Z = \int \mathrm{d}\boldsymbol{m} \exp(B : \boldsymbol{m}\boldsymbol{m}).$$

In the above, Q ranges over the set that consists of all the symmetric trace-one matrices whose eigenvalues are restricted to $(0, 1)$. The set turns out to be all the possible averages of $\boldsymbol{m}\boldsymbol{m}$ under continuous measures.

$$\left\{ Q = \int \mathrm{d}\boldsymbol{m} \; \boldsymbol{m}\boldsymbol{m} \rho(\boldsymbol{m}) : \rho : S^2 \to \mathbb{R}^2, \rho(\boldsymbol{m}) \geq 0, \int \rho(\boldsymbol{m}) = 1 \right\}.$$

A natural extension will be minimizing the entropy term with given $(\boldsymbol{p}, Q_1, Q_2)$.

$$\begin{aligned} & \inf \int_{SO_3} \mathrm{d}\nu \rho(P) \log \rho(P), \\ \text{s.t.} \quad & \int \mathrm{d}\nu \rho(P) = 1, \\ & \int \mathrm{d}\nu \boldsymbol{m}_1 \rho(P) = \boldsymbol{p}, \\ & \int \mathrm{d}\nu \boldsymbol{m}_1 \boldsymbol{m}_1 \rho(P) = Q_1, \\ & \int \mathrm{d}\nu \boldsymbol{m}_2 \boldsymbol{m}_2 \rho(P) = Q_2. \end{aligned}$$

The Euler-Lagrange equation gives

$$\rho(P) = \frac{1}{Z}\exp(\boldsymbol{b}\cdot\boldsymbol{m}_1 + B_1 : \boldsymbol{m}_1\boldsymbol{m}_1 + B_2 : \boldsymbol{m}_2\boldsymbol{m}_2), \tag{2.10}$$

where $\boldsymbol{b}$ is a vector, B_1 and B_2 are symmetric matrices, and

$$Z = \int \mathrm{d}\nu \exp(\boldsymbol{b}\cdot\boldsymbol{m}_1 + B_1 : \boldsymbol{m}_1\boldsymbol{m}_1 + B_2 : \boldsymbol{m}_2\boldsymbol{m}_2).$$

It is straightforward to check that if $(\boldsymbol{b}, B_1, B_2)$ solves the minimization problem for $(\boldsymbol{p}, Q_1, Q_2)$, then $(T\boldsymbol{b}, TB_1T^T, TB_2T^T)$ solves it for $(T\boldsymbol{p}, TQ_1T^T, TQ_2T^T)$ for any $T \in SO_3$. For example,

$$\begin{aligned}
&\int \mathrm{d}\nu \boldsymbol{m}_1 \frac{1}{Z}\exp(T\boldsymbol{b}\cdot\boldsymbol{m}_1 + TB_1T^T : \boldsymbol{m}_1\boldsymbol{m}_1 + TB_2T^T : \boldsymbol{m}_2\boldsymbol{m}_2) \\
&\quad= \int \mathrm{d}\nu \boldsymbol{m}_1 \frac{1}{Z}\exp(\boldsymbol{b}\cdot T^T\boldsymbol{m}_1 + B_1 : (T^T\boldsymbol{m}_1)(T^T\boldsymbol{m}_1) + B_2 : (T^T\boldsymbol{m}_2)(T^T\boldsymbol{m}_2)) \\
&\quad= \int \mathrm{d}\nu (T\boldsymbol{m}_1) \frac{1}{Z}\exp(\boldsymbol{b}\cdot\boldsymbol{m}_1 + B_1 : \boldsymbol{m}_1\boldsymbol{m}_1 + B_2 : \boldsymbol{m}_2\boldsymbol{m}_2) \\
&\quad= T\boldsymbol{p}.
\end{aligned}$$

One might demand that $\boldsymbol{p}$, Q_1 and Q_2 range over all the possible averages like in the Bingham closure. However, this would generate too many degrees of freedom. Here we also refer to the results of homogeneous phases. We find that Q_1 and Q_2 can be diagonalized simultaneously, and have proved that in this case $\boldsymbol{p}$ is one of the eigenvectors of Q_1 and Q_2 [15]. For this reason, we demand that there exists a $T \in SO_3$ such that

$$\begin{aligned}
\boldsymbol{p} &= T(s, 0, 0)^T, \\
Q_1 &= T\mathrm{diag}(q_{11}, q_{12}, q_{13})T^T, \\
Q_2 &= T\mathrm{diag}(q_{21}, q_{22}, q_{23})T^T,
\end{aligned}$$

where $q_{i3} = 1 - q_{i1} - q_{i2}$. Or equivalently,

$$\begin{aligned}
\boldsymbol{p} &= s\boldsymbol{n}_1, \\
Q_1 &= q_{11}\boldsymbol{n}_1\boldsymbol{n}_1 + q_{12}\boldsymbol{n}_2\boldsymbol{n}_2 + q_{13}\boldsymbol{n}_3\boldsymbol{n}_3, \\
Q_2 &= q_{21}\boldsymbol{n}_1\boldsymbol{n}_1 + q_{22}\boldsymbol{n}_2\boldsymbol{n}_2 + q_{23}\boldsymbol{n}_3\boldsymbol{n}_3
\end{aligned}$$

with $(\boldsymbol{n}_1, \boldsymbol{n}_2, \boldsymbol{n}_3) = (\boldsymbol{e}_1, \boldsymbol{e}_2, \boldsymbol{e}_3)T$. We will prove that the scalars above shall satisfy

$$\begin{aligned}
q_{ij} &> 0, \\
q_{11} + q_{12} &< 1, \\
q_{11} + q_{21} &< 1, \\
q_{12} + q_{22} &< 1, \\
q_{21} + q_{22} &< 1, \\
q_{11} + q_{12} + q_{21} + q_{22} &> 1, \\
s^2 &< q_{11}.
\end{aligned} \tag{2.11}$$

Furthermore, we will show that when $T = I$, for any (s, q_{ij}) satisfying the above constraints, there exists a $(\boldsymbol{b}, B_1, B_2)$ of the form

$$\begin{aligned}
\boldsymbol{b} &= (b_1, 0, 0)^T, \\
B_1 &= \mathrm{diag}(b_{11}, b_{12}, 0), \\
B_2 &= \mathrm{diag}(b_{21}, b_{22}, 0),
\end{aligned} \tag{2.12}$$

such that (2.10) solves the minimization problem uniquely. The proof is left to Appendix.

2.3 The elastic energy

To write down the elastic energy in terms of tensors, we aim to find an approximation of $M^{(k)}$ that consists of terms of the following form.

$$\begin{aligned}&p_{i_1j_1}\dots p_{i_rj_r}(\boldsymbol{m}_{l_1}\dots\boldsymbol{m}_{l_s}\boldsymbol{m}'_{l_{s+1}}\dots\boldsymbol{m}'_{l_t}\underbrace{I\dots I}_{(k-t)/2})_{\rm sym}\\ =&\Big([m_{i_1\sigma_1}\dots m_{i_r\sigma_r}\boldsymbol{m}_{l_1}\dots\boldsymbol{m}_{l_s}][m'_{j_1\sigma_1}\dots m'_{j_r\sigma_r}\boldsymbol{m}'_{l_{s+1}}\dots\boldsymbol{m}'_{l_t}]\underbrace{I\dots I}_{(k-t)/2}\Big)_{\rm sym},\end{aligned}\tag{2.13}$$

where we use the notation $\boldsymbol{m}'_i=\boldsymbol{m}_i(P')$, and $M_{\rm sym}$ to denote the permutational average of a tensor M.

$$(M_{\rm sym})_{l_1\dots l_k}=\frac{1}{k!}\sum_\sigma M_{l_{\sigma(1)}\dots l_{\sigma(k)}}.$$

A term (2.13) in the approximation of $M^{(k)}$ yields the following term in the elastic energy.

$$(c(x)\langle m_{i_1\sigma_1}\dots m_{i_r\sigma_r}m_{l_1\tau_1}\dots m_{l_s\tau_s}\rangle)\Delta^{(k-t)/2}\partial_{\tau_1}\dots\partial_{\tau_t}(c(x)\langle m_{j_1\sigma_1}\dots m_{j_r\sigma_r}m_{l_{s+1}\tau_{s+1}}\dots m_{l_t\tau_t}\rangle).\tag{2.14}$$

First we express $M^{(k)}$ in the form of separated variables. The generic form reads

$$M^{(k)}(P,P')=\sum c_{l_1\dots l_s;l_{s+1}\dots l_t;(k-t)/2}(\boldsymbol{m}_{l_1}\dots\boldsymbol{m}_{l_s}\boldsymbol{m}'_{l_{s+1}}\dots\boldsymbol{m}'_{l_t}\underbrace{I\dots I}_{(k-t)/2})_{\rm sym},\tag{2.15}$$

where the sum is taken over $0\le s\le t\le k$ and $l_u=1,2,3$. The coefficients $c_{l_1\dots l_s,l_{s+1}\dots l_k}$ are functions of $\bar P$. This is because

$$M^{(k)}(TP,TP')_{i_1\dots i_k}=T_{i_1j_1}\dots T_{i_kj_k}M^{(k)}(P,P')_{j_1\dots j_k},\ \forall T\in SO_3,\tag{2.16}$$

which origins from

$$G(T\boldsymbol{r},TP,TP')=G(\boldsymbol{r},P,P').$$

Actually,

$$\begin{aligned}&M^{(k)}(TP,TP')_{i_1\dots i_k}\\ =&T_{i_1j_1}\dots T_{i_kj_k}M^{(k)}(P,P')_{j_1\dots j_k}\\ =&\sum c_{l_1\dots l_s;l_{s+1}\dots l_t;(k-t)/2}\frac{1}{k!}\sum_\sigma T_{i_{\sigma(1)}j_1}m_{l_1j_1}(P)\dots T_{i_{\sigma(s)}j_s}m_{l_sj_s}(P)\\ &T_{i_{\sigma(s+1)}j_{s+1}}m_{l_{s+1}j_{s+1}}(P')\dots T_{i_{\sigma(t)}j_t}m_{l_tj_t}(P')\\ &(\delta_{i_{\sigma(t+1)}j_{t+1}}\delta_{j_{t+1}j_{t+2}}\delta_{i_{\sigma(t+2)}j_{t+2}})\dots(\delta_{i_{\sigma(k-1)}j_{k-1}}\delta_{j_{k-1}j_k}\delta_{i_{\sigma(k)}j_k}).\\ =&\sum c_{l_1\dots l_s;l_{s+1}\dots l_t;(k-t)/2}[(\boldsymbol{m}_{l_1}(TP)\dots\boldsymbol{m}_{l_s}(TP)\boldsymbol{m}_{l_{s+1}}(TP')\dots\boldsymbol{m}_{l_t}(TP')\underbrace{I\dots I}_{(k-t)/2})_{\rm sym}]_{i_1\dots i_k}.\end{aligned}$$

Furthermore, from

$$M^{(k)}(P',P)=(-1)^kM^{(k)}(P,P'),\tag{2.17}$$

we deduce that

$$c_{l_1\dots l_s;l_{s+1}\dots l_t;(k-t)/2}(\bar P)=(-1)^kc_{l_{s+1}\dots l_t;l_1\dots l_s;(k-t)/2}(\bar P^T).\tag{2.18}$$

There is one thing to be clarified. Because the representation (2.15) is not unique, the equality like (2.18) means that we can choose an appropriate representation whose coefficients satisfy it. Take

(2.18) as an example. From (2.17), we know that

$$\begin{aligned} M^{(k)}(P,P') &= (-1)^k M^{(k)}(P',P) \\ &= \sum (-1)^k c_{l_1\dots l_s;l_{s+1}\dots l_t;(k-t)/2}(\bar{P}^T)(\boldsymbol{m}'_{l_1}\dots\boldsymbol{m}'_{l_s}\boldsymbol{m}_{l_{s+1}}\dots\boldsymbol{m}_{l_t}\underbrace{I\dots I}_{(k-t)/2})_{\rm sym} \\ &= \sum (-1)^k c_{l_{s+1}\dots l_t;l_1\dots l_s;(k-t)/2}(\bar{P}^T)(\boldsymbol{m}_{l_1}\dots\boldsymbol{m}_{l_s}\boldsymbol{m}'_{l_{s+1}}\dots\boldsymbol{m}'_{l_t}\underbrace{I\dots I}_{(k-t)/2})_{\rm sym}. \end{aligned}$$

Thus we can find an alternative representation by substituting $c_{l_1\dots l_s;l_{s+1}\dots l_t;(k-t)/2}$ with

$$\tilde{c}_{l_1\dots l_s;l_{s+1}\dots l_t;(k-t)/2}(\bar{P}) = \frac{1}{2}\left[(-1)^k c_{l_{s+1}\dots l_t;l_1\dots l_s;(k-t)/2}(\bar{P}^T) + c_{l_1\dots l_s;l_{s+1}\dots l_t;(k-t)/2}(\bar{P})\right]$$

in (2.15). The new coefficients $\tilde{c}_{l_1\dots l_s;l_{s+1}\dots l_t;(k-t)/2}$ satisfy (2.18). From now on, we omit this kind of deduction and present only the results.

The representation (2.15) can be simplified due to molecular symmetry. For molecules with the symmetry plane $\hat{O}\boldsymbol{m}_1\boldsymbol{m}_2$, the representation (2.15) contains only terms with $l_u = 1, 2$.

$$(\boldsymbol{m}_{l_1}\dots\boldsymbol{m}_{l_s}\boldsymbol{m}'_{l_{s+1}}\dots\boldsymbol{m}'_{l_t}\underbrace{I\dots I}_{(k-t)/2})_{\rm sym}, \quad l_u = 1, 2. \tag{2.19}$$

Actually, $M^{(k)}$ can always be represented by the bases

$$(\boldsymbol{m}_{i_1}\dots\boldsymbol{m}_{i_k})_{\rm sym}, \quad i_k = 1, 2, 3. \tag{2.20}$$

If $\boldsymbol{m}'_3 \neq \pm\boldsymbol{m}_3$, $\boldsymbol{m}_3$ can be represented by $\{\boldsymbol{m}_i, \boldsymbol{m}'_i\}$, $i = 1, 2$. Thus the bases $(\boldsymbol{m}_{i_1}\dots\boldsymbol{m}_{i_k})_{\rm sym}$ can be represented. Otherwise $\boldsymbol{m}'_3 = \pm\boldsymbol{m}_3$. By reflection symmetry, the components in (2.20) with odd number of $\boldsymbol{m}_3$ are zero. Since $\boldsymbol{m}_3\boldsymbol{m}_3 = I - \boldsymbol{m}_1\boldsymbol{m}_1 - \boldsymbol{m}_2\boldsymbol{m}_2$, components with even number of $\boldsymbol{m}_3$ can be represented.

The coefficient of each term in the representation (2.19) can be reduced to a function of $(p_{11}, p_{12}, p_{21}, p_{22})$. Suppose we have a representation

$$M^{(k)}(P,P') = \sum c_{l_1\dots l_s;l_{s+1}\dots l_t;(k-t)/2}(\bar{P})(\boldsymbol{m}_{l_1}\dots\boldsymbol{m}_{l_s}\boldsymbol{m}'_{l_{s+1}}\dots\boldsymbol{m}'_{l_t}\underbrace{I\dots I}_{(k-t)/2})_{\rm sym}.$$

Let $J = \mathrm{diag}(-1, -1, 1)$. Note that $\boldsymbol{m}_i(PJ) = -\boldsymbol{m}_i(P)$ for $i = 1, 2$, and that $k - t$ is even. By

$$M^{(k)}(PJ, P'J) = (-1)^k M^{(k)}(P,P'), \tag{2.21}$$

we have

$$c_{l_1\dots l_s;l_{s+1}\dots l_t;(k-t)/2}(\bar{P}) = c_{l_1\dots l_s;l_{s+1}\dots l_t;(k-t)/2}(J\bar{P}J) = c_{l_1\dots l_s;l_{s+1}\dots l_t;(k-t)/2}(p_{11}, p_{12}, p_{21}, p_{22}).$$

Now just note that $\bar{P}$ and $J\bar{P}J$ are the only two elements in SO_3 with given $(p_{11}, p_{12}, p_{21}, p_{22})$.

The C_{2v} symmetry of bent-core molecules exposes some conditions on the coefficients. Let $J_1 = \mathrm{diag}(1, -1, -1)$, we have

$$M^{(k)}(P,P') = M^{(k)}(PJ_1, P') = M^{(k)}(P, P'J_1). \tag{2.22}$$

Thus

$$\begin{aligned} &c_{l_1\dots l_s;l_{s+1}\dots l_t;(k-t)/2}(\bar{P}) \\ &\quad = (-1)^{\#\{u|l_u=2,u=1,\dots s\}} c_{l_1\dots l_s;l_{s+1}\dots l_t;(k-t)/2}(J_1\bar{P}) \\ &\quad = (-1)^{\#\{u|l_u=2,u=s+1,\dots t\}} c_{l_1\dots l_s;l_{s+1}\dots l_t;(k-t)/2}(\bar{P}J_1), \end{aligned} \tag{2.23}$$

where $\#A$ denotes the number of elements in the set A.

Next we use a polynomial to approximate $c_{l_1\dots l_s;l_{s+1}\dots l_t;(k-t)/2}(p_{11},p_{12},p_{21},p_{22})$.

$$c_{l_1\dots l_s;l_{s+1}\dots l_t;(k-t)/2}(p_{11},p_{12},p_{21},p_{22})=\sum c^{i_1\dots i_r;j_1\dots j_r}_{l_1\dots l_s;l_{s+1}\dots l_t;(k-t)/2}p_{i_1j_1}\dots p_{i_rj_r}, \tag{2.24}$$

where $i_u,j_u,l_u=1,2$. taking (2.24) into the representation (2.15), we obtain an approximation of $M^{(k)}$, denoted by $\hat{M}^{(k)}$. The properties of $M^{(k)}$ should be inherited by $\hat{M}^{(k)}$. By (2.18), we have

$$c^{i_1\dots i_r;j_1\dots j_r}_{l_1\dots l_s;l_{s+1}\dots l_t;(k-t)/2}=(-1)^k c^{j_1\dots j_r;i_1\dots i_r}_{l_{s+1}\dots l_t;l_1\dots l_s;(k-t)/2}. \tag{2.25}$$

And by (2.23), we have

$$\begin{aligned}
&c^{i_1\dots i_r;j_1\dots j_r}_{l_1\dots l_s;l_{s+1}\dots l_t;(k-t)/2}\\
=&(-1)^{\#\{u|l_u=2,u=1,\dots s\}+\#\{u|i_u=2,u=1,\dots r\}}c^{i_1\dots i_r;j_1\dots j_r}_{l_1\dots l_s;l_{s+1}\dots l_t;(k-t)/2}\\
=&(-1)^{\#\{u|l_u=2,u=s+1,\dots t\}+\#\{u|j_u=2,u=1,\dots r\}}c^{i_1\dots i_r;j_1\dots j_r}_{l_1\dots l_s;l_{s+1}\dots l_t;(k-t)/2}.
\end{aligned} \tag{2.26}$$

Therefore the approximation (2.24) contains only terms such that the value two appears even times in both $(i_1,\dots i_r,l_1\dots l_s)$ and $(j_1,\dots j_r,l_{s+1}\dots l_t)$.

Based on the analysis, we write down all the terms in $\hat{M}^{(1)}$ and $\hat{M}^{(2)}$. We truncate them at $r+\max\{s,t-s\}\le 2$, which restrains the moments to those no more than second order.

$$\begin{aligned}
\hat{M}^{(1)}=&-c_{10}(\boldsymbol{m}_1-\boldsymbol{m}_1')-c_{11}p_{11}(\boldsymbol{m}_1-\boldsymbol{m}_1')-c_{12}(p_{21}\boldsymbol{m}_2-p_{12}\boldsymbol{m}_2'),\\
\hat{M}^{(2)}=&-\left(c_{20}+c_{21}p_{11}+c_{22}p_{11}^2+c_{23}p_{22}^2+c_{24}(p_{12}^2+p_{21}^2)\right)I\\
&-c_{25}(\boldsymbol{m}_1\boldsymbol{m}_1+\boldsymbol{m}_1'\boldsymbol{m}_1')-c_{26}(\boldsymbol{m}_2\boldsymbol{m}_2+\boldsymbol{m}_2'\boldsymbol{m}_2')\\
&-(c_{27}+c_{28}p_{11})(\boldsymbol{m}_1\boldsymbol{m}_1'+\boldsymbol{m}_1'\boldsymbol{m}_1)-c_{29}p_{22}(\boldsymbol{m}_2\boldsymbol{m}_2'+\boldsymbol{m}_2'\boldsymbol{m}_2)\\
&-c_{2,10}\left[p_{12}(\boldsymbol{m}_1\boldsymbol{m}_2'+\boldsymbol{m}_2'\boldsymbol{m}_1)+p_{21}(\boldsymbol{m}_2\boldsymbol{m}_1'+\boldsymbol{m}_1'\boldsymbol{m}_2)\right].
\end{aligned}$$

Thus the total free energy is written as follows. Here we have done several integrations by parts and discarded surface terms. They vanish under the periodic boundary condition.

$$\begin{aligned}
\frac{F[c,Q_1,Q_2,\boldsymbol{p}]}{k_BT}=\frac{1}{V}\int \mathrm{d}\boldsymbol{x}\Big\{&c(\boldsymbol{b}\cdot\boldsymbol{p}+B_1:Q_1+B_2:Q_2-\log Z)\\
&+\frac{1}{2}(c_{00}c^2+c_{01}|c\boldsymbol{p}|^2+c_{02}|cQ_1|^2+c_{03}|cQ_2|^2+2c_{04}cQ_1:cQ_2)\\
&+c_{10}c\partial_ip_i+c_{11}cp_j\partial_i(cQ_{1ij})+c_{12}cp_j\partial_i(cQ_{2ij})\\
&+\frac{1}{4}\big[c_{20}|\nabla c|^2+c_{21}|\nabla(c\boldsymbol{p})|^2+c_{22}|\nabla(cQ_1)|^2+c_{23}|\nabla(cQ_2)|^2\\
&+2c_{24}\partial_i(cQ_{1jk})\partial_i(cQ_{2jk})+2c_{25}\partial_ic\partial_j(cQ_{1ij})+2c_{26}\partial_ic\partial_j(cQ_{2ij})\\
&+2c_{27}(\partial_i(cp_i))^2+2c_{28}|\partial_i(cQ_{1ik})|^2+2c_{29}|\partial_i(cQ_{2ik})|^2\\
&+4c_{2,10}\partial_i(cQ_{1ik})\cdot\partial_j(cQ_{2jk})\big]\Big\}.
\end{aligned} \tag{2.27}$$

For nematic phases, by letting c be constant in space, we get (1.1).

2.4 The derivation of coefficients

In the above, we have determined the approximation form of $M^{(k)}(P,P')$. Denote it by $\hat{M}^{(k)}(P,P')$. Its coefficients are obtained by fitting. The method of fitting is certainly not unique. Here we choose to minimize the distance between $M^{(k)}$ and its approximation, which is given by

$$||M^{(k)}-\hat{M}^{(k)}||^2=\int_{SO_3}d\nu(\bar{P})||M^{(k)}(P,P')-\hat{M}^{(k)}(P,P')||_F^2, \tag{2.28}$$

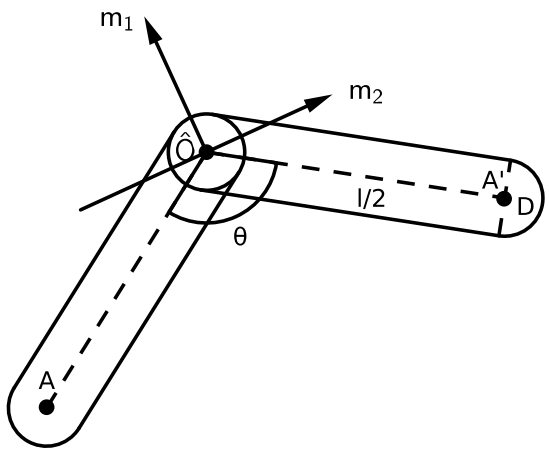

Figure 2: A bent-core molecule that consists of spheres of diameter D. The sphere centers are distributed on the broken line $A\hat{O}A'$ with $A\hat{O} = \hat{O}A' = l/2$ and $\angle A\hat{O}A' = \theta$.

where $||\cdot||_F$ is the Frobenius norm,

$$||M||_F^2 = \sum_{i_1 \dots i_k} |M_{i_1 \dots i_k}|^2. \tag{2.29}$$

The distance is well-defined, for

$$\begin{aligned} ||M^{(k)}(TP, TP') - \hat{M}^{(k)}(TP, TP')||_F^2 =& ||T_{j_1 i_1} \dots T_{j_k i_k} (M^{(k)}_{i_1 \dots i_k}(P, P') - \hat{M}^{(k)}_{i_1 \dots i_k}(P, P'))||_F^2 \\ =& ||M^{(k)}(P, P') - \hat{M}^{(k)}(P, P')||_F^2. \end{aligned}$$

The fitting is a standard least-square problem. What is remaining is the calculation of $M^{(k)}(P, P')$. In Appendix we will derive expressions for them when adopting the hardcore potential. We regard a bent-core molecule as consisting of spheres of diameter D, whose centers spread over a two-segment broken line forming an angle θ with each segment $l/2$ in length, which is drawn in Fig.2. There are two molecular parameters reflecting the shape: $D/l, \theta$. The derived coefficients are proportional to l^3 that can be merged with c. In the following, we still use c in the place of cl^3.

To ensure the lower-boundedness of the free energy, the coefficients must be located in a certain range. However, it is difficult to figure out the whole range. So we adopt a range possibly rather strict.

$$\begin{aligned} & c_{24}^2 < c_{22} c_{23}, \\ & (2c_{2,10} + c_{24})^2 < (2c_{28} + c_{22})(2c_{29} + c_{23}), \\ & c_{21}, c_{22}, c_{23}, c_{27}, 2c_{28} + c_{22}, 2c_{29} + c_{23} > 0. \end{aligned}$$

Under these restrictions, the second-order elastic energy is positive definite, for we can rewrite it as follows.

$$\begin{aligned} & \frac{1}{4}\big[c_{21}|\nabla \boldsymbol{p}|^2 + c_{25}(\partial_i p_i)^2 + \frac{1}{2} c_{22} |\partial_i Q_{1jk} - \partial_j Q_{1ik}|^2 \\ & + \frac{1}{2} c_{23} |\partial_i Q_{2jk} - \partial_j Q_{2ik}|^2 + c_{24}(\partial_i Q_{1jk} - \partial_j Q_{1ik})(\partial_i Q_{2jk} - \partial_j Q_{2ik}) \\ & + (2c_{28} + c_{22})|\partial_i Q_{1ik}|^2 + (2c_{29} + c_{23})|\partial_i Q_{2ik}|^2 + 2(2c_{2,10} + c_{24}) \partial_i Q_{1ik} \cdot \partial_j (Q_{2jk})\big]. \end{aligned}$$

Here we have done some integrations by parts and used the equality

$$\partial_i A_{jk}\partial_i B_{jk} - \partial_i A_{jk}\partial_j B_{ik} = \frac{1}{2}(\partial_i A_{jk} - \partial_j A_{ik})(\partial_i B_{jk} - \partial_j B_{ik}).$$

Moreover, it controls the first-order elastic energy, for we can choose a C large enough such that the matrix below is positive definite.

$$\begin{pmatrix} c_{28} + \frac{1}{2}c_{22} & c_{2,10} + \frac{1}{2}c_{24} & c_{11} \\ c_{2,10} + \frac{1}{2}c_{24} & c_{29} + \frac{1}{2}c_{23} & c_{12} \\ c_{11} & c_{12} & c_{01} + C \end{pmatrix}.$$

Thus

$$\begin{aligned}\frac{F[Q_1, Q_2, \boldsymbol{p}]}{k_B T} \geq \frac{1}{V}\int \mathrm{d}\boldsymbol{x}\Big[c(\boldsymbol{b}\cdot\boldsymbol{p} + B_1 : Q_1 + B_2 : Q_2 - \log Z) \\ + \frac{c^2}{2}\big((c_{01} - C)|\boldsymbol{p}|^2 + c_{02}|Q_1|^2 + c_{03}|Q_2|^2 + 2c_{04}Q_1 : Q_2\big)\Big].\end{aligned}$$

Each term in the second line is bounded. The first line is also lower-bounded from the strict convexity of the entropy.

The coefficients derived from the molecular parameters do not lie in the range and the numerical experiments show signs of lower-unboundedness. There are two possible reasons for the improperness of the coefficients. One is that the least square fitting may not be good enough. Other methods of approximation may work better. The other is that the molecule may prefer smectic phases under the parameters, which calls for higher-order terms to stabilize the free energy. Nevertheless, we will do a few modifications to make the coefficients lie in the range.

The first-order elastic energy is crucial to the appearance of modulated phases. Actually, if

$$\begin{pmatrix} c_{28} + \frac{1}{2}c_{22} & c_{2,10} + \frac{1}{2}c_{24} & c_{11} \\ c_{2,10} + \frac{1}{2}c_{24} & c_{29} + \frac{1}{2}c_{23} & c_{12} \\ c_{11} & c_{12} & c_{01} + \frac{1}{c^2} \end{pmatrix}$$

is positive definite, only spatially homogeneous phases will be stable. In this case, actually,

$$\begin{aligned}\frac{F[Q_1, Q_2, \boldsymbol{p}]}{k_B T} \geq \frac{1}{V}\int \mathrm{d}\boldsymbol{x}\Big[c(\boldsymbol{b}\cdot\boldsymbol{p} + B_1 : Q_1 + B_2 : Q_2 - \log Z) \\ - |\boldsymbol{p}|^2 + \frac{c^2}{2}(c_{02}|Q_1|^2 + c_{03}|Q_2|^2 + 2c_{04}Q_1 : Q_2)\Big].\end{aligned}$$

We have proved in [15] that the minimum of the right side of the inequality satisfies $\boldsymbol{p} = 0$. This implies that it is also the minimum of the free energy. When $c_{01} > 0$, the matrix above is positive definite for $c_{11}, c_{12} = 0$. Since a small perturbation retains the positive definiteness, for small c_{11}, c_{12}, only spatially homogeneous phases appear. Alternatively, when c_{01} is large enough, the above matrix is also positive definite, which eliminates $\boldsymbol{p}$ as well. This would occur if the antiferroelectricity is large. The electromagnetic interaction is beyond our consideration in the current work and needs further discussion.

3 Results and discussion

In this section, we examine the phases where inhomogeneity occurs only in the x-direction. Now the free energy becomes

$$\begin{aligned}\frac{F[Q_1,Q_2,\boldsymbol{p}]}{k_BT} = \frac{1}{L}\int \mathrm{d}x\Big\{ & c(\boldsymbol{b}\cdot\boldsymbol{p} + B_1 : Q_1 + B_2 : Q_2 - \log Z) \\ & \frac{c^2}{2}(c_{01}|\boldsymbol{p}|^2 + c_{02}|Q_1|^2 + c_{03}|Q_2|^2 + 2c_{04}Q_1 : Q_2) \\ & + c^2(c_{11}p_j\frac{\mathrm{d}}{\mathrm{d}x}Q_{1,1j} + c_{12}p_j\frac{\mathrm{d}}{\mathrm{d}x}Q_{2,1j}) \\ & + \frac{c^2}{4}\big[c_{21}|\frac{\mathrm{d}}{\mathrm{d}x}\boldsymbol{p}|^2 + c_{22}|\frac{\mathrm{d}}{\mathrm{d}x}Q_1|^2 + c_{23}|\frac{\mathrm{d}}{\mathrm{d}x}Q_2|^2 + 2c_{24}\frac{\mathrm{d}}{\mathrm{d}x}Q_{1jk} : \frac{\mathrm{d}}{\mathrm{d}x}Q_{2jk} \\ & + 2c_{27}(\frac{\mathrm{d}}{\mathrm{d}x}p_1)^2 + 2c_{28}|\frac{\mathrm{d}}{\mathrm{d}x}Q_{1,1k}|^2 \\ & + 2c_{29}|\frac{\mathrm{d}}{\mathrm{d}x}Q_{2,1k}|^2 + 4c_{2,10}\frac{\mathrm{d}}{\mathrm{d}x}Q_{1,1k}\cdot\frac{\mathrm{d}}{\mathrm{d}x}Q_{2,1k}\big]\Big\}. \end{aligned} \tag{3.1}$$

To find modulated phases, we need to minimize the free energy under the periodic boundary condition about the tensors and the length of period L.

$$\min_{\boldsymbol{p}(x),Q_1(x),Q_2(x),L} F.$$

We use finite volume method to discretize the free energy. Generally speaking, in $[x_k, x_{k+1}]$, a function $f(x)$ is approximated by $\frac{1}{2}(f(x_k)+f(x_{k+1}))$, and its derivative is approximated by $\frac{1}{x_{k+1}-x_k}(f(x_{k+1})-f(x_k))$. For example, the term

$$\int_{x_k}^{x_{k+1}} \mathrm{d}x p_i \frac{\mathrm{d}}{\mathrm{d}x}Q_{1,1i}$$

is approximated by

$$(x_{k+1}-x_k)\cdot\frac{p_i(x_{k+1})+p_i(x_k)}{2}\cdot\frac{Q_{1,1i}(x_k)-Q_{1,1i}(x_{k+1})}{x_{k+1}-x_k}.$$

The tensors are represented by their eigenvalues and co-owned local orientation $T(x)$.

$$\begin{aligned}\boldsymbol{p}(x) &= T(x)(s(x),0,0)^T, \\ Q_1(x) &= T(x)\mathrm{diag}(q_{11}(x),q_{12}(x),q_{13}(x))T(x)^T, \\ Q_2(x) &= T(x)\mathrm{diag}(q_{21}(x),q_{22}(x),q_{23}(x))T(x)^T.\end{aligned}$$

$T(x)$ is represented by the Euler angles $(\alpha(x),\beta(x),\gamma(x))$ as in (2.1). The magnitudes are calculated from (b_1, b_{ij}) using (2.10) and (2.12).

3.1 The phase diagram of the homogeneous phases

Before looking at the modulated phases, we give a phase diagram of homogeneous phases in the absence of the elastic energy. From the comment in the previous section, it is equivalent to the case where c_{11} and c_{12} are small enough or c_{01} is large enough. The phase diagram generated by F_{bulk} in the tensor model is drawn in Fig.3. We also examine the third-order bulk energy (2.8). When adopting the third-order bulk energy, we no longer handle the entropy term with the closure we introduce, but solve it directly. Here we need to solve a set of self-consistent equations about the following five angular moments [15].

$$\left\{ \langle \boldsymbol{m}_1 \rangle, \langle \boldsymbol{m}_1\boldsymbol{m}_1 \rangle, \langle \boldsymbol{m}_2\boldsymbol{m}_2 \rangle, \langle \boldsymbol{m}_1\boldsymbol{m}_1\boldsymbol{m}_1 \rangle, \langle \boldsymbol{m}_1\boldsymbol{m}_2\boldsymbol{m}_2 \rangle \right\}.$$

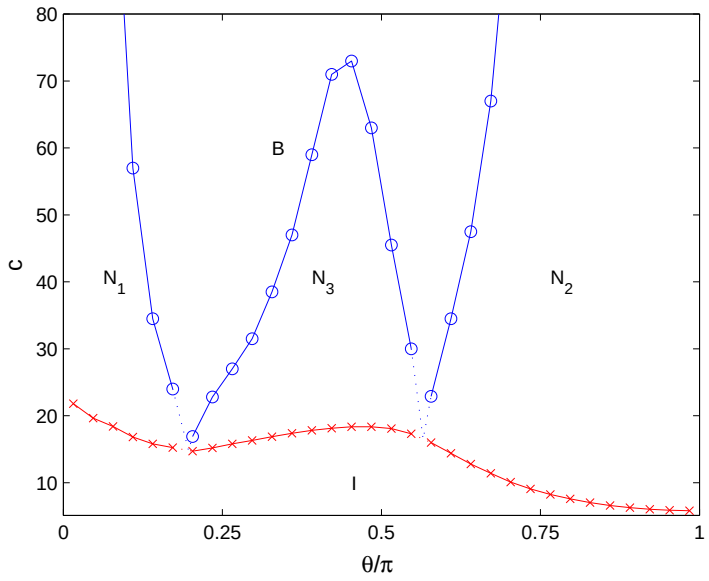

Figure 3: Phase diagram of F_{bulk} about c and θ. Five phases are found stable: isotropic phase(I), uniaxial nematic phase about $\boldsymbol{m}_i$ (N_i), and biaxial nematic phase(B). The dotted lines are plotted based on speculation.

With the derived coefficients from molecular parameters, we find that the first-order and the third-order tensors vanish. Moreover, Q_1 and Q_2 always share one eigenframe. Since the derived c_{02}, c_{03} and c_{04} are equal in (2.7) and in (2.8), the homogeneous phases obtained from (2.8) are identical to those obtained from the free energy (1.1).

The classification of phases has been discussed in [15] and is briefly described here. It is based on the uniaxiality of Q_1 as well as Q_2.

- Isotropic phase. $Q_1 = Q_2 = \frac{I}{3}$.
- Uniaxial nematic phase. Both Q_1 and Q_2 are uniaxial with the same axis. For further classification, we examine at the same time $Q_3 = \langle \boldsymbol{m}_3 \boldsymbol{m}_3 \rangle = I - Q_1 - Q_2$. Suppose that

$$Q_i = s_i(\boldsymbol{n}\boldsymbol{n} - \frac{I}{3}) + \frac{I}{3}, \quad i = 1, 2, 3.$$

  We find that only one of the s_i can be positive. The case $s_i > 0$ is represented by N_i, which means $\boldsymbol{m}_i$ aligns near the axis $\pm\boldsymbol{n}$, and the other two $\boldsymbol{m}_i$ tend to align in the plane perpendicular to this axis.

- Biaxial nematic phase. Both Q_1 and Q_2 are biaxial.

Since $\boldsymbol{p}$ is zero, the bulk energy is reduced to

$$\frac{c^2}{2}(c_{02}|Q_1|^2 + c_{03}|Q_2|^2 + 2c_{04}Q_1 : Q_2).$$

From the phase diagram, we know that with the increase of c, the I-N_i-B sequences ($i = 1, 2, 3$) are obtained. It is likely that I-B transition will occur at the border of two I-N_i-B regions. As this is not the focus of the current work, we do not try to examine it thoroughly but point out a series of papers where the related topics have been discussed [21, 22].

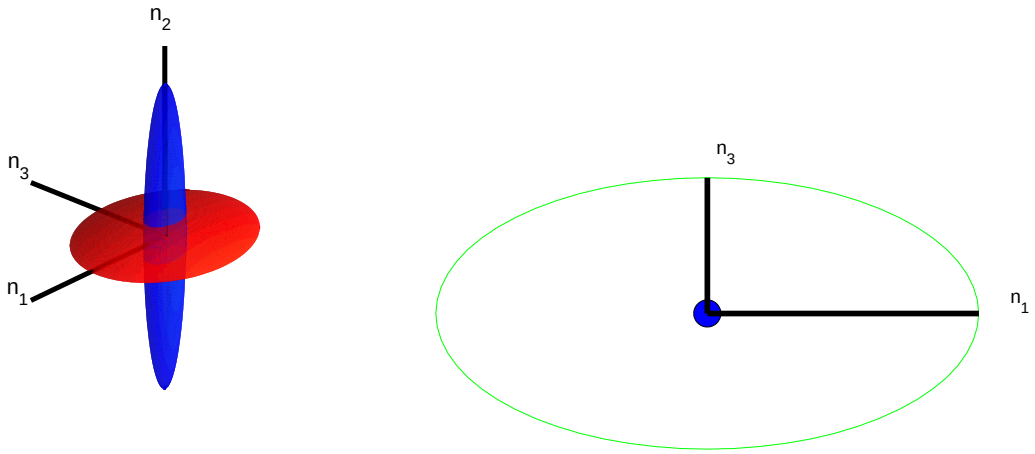

Figure 4: The representation of Q_1 and Q_2 when q_{22} is very large, typically $q_{22} > 0.8$. Left: the plot of Q_1 (red) and Q_2 (blue), represented by ellipsoid whose axes are proportional to the eigenvalues. Right: The simplified representation, where Q_2 is reduced to an axis and Q_1 is reduced to an ellipse (drawn in green) in the plane $\boldsymbol{n}_1$-$\boldsymbol{n}_3$.

3.2 Modulated phases

Fix

$$c_1 = 0.002661, c_2 = -0.039939, c_3 = -0.843494, c_4 = -0.193564;$$
$$c_{21} = 0.026175, c_{22} = 0.020829, c_{23} = 0.105702, c_{24} = 0.020472,$$
$$c_{25} = 0.064102, c_{26} = 0.017482, c_{27} = 0.182341, c_{28} = 0.034809.$$

The coefficients are derived from $\theta = \frac{45\pi}{64}$, $D/l = 0.1$, with modification to c_{23}, c_{26}, c_{27}. Let $c_{11}^{(0)} = 0.389636$ and $c_{12}^{(0)} = 0.389919$. They are shrunken to 1/10 of the derived values with their signs retained. We will examine a few values of c_{1i} near $c_{1i}^{(0)}$.

Before presenting the phases, we first look at how the tensors reflect the alignment of molecules. In our choice of coefficients for the bulk energy, it is very likely that one of q_{2i} is greatly large than the other two. We choose $T(x)$ such that $q_{22} \gg q_{21}, q_{23}$. Actually, all the results we will present meet this condition and q_{2i} fluctuate little in space. If we draw an ellipsoid with its axes equal to the eigenvalues of a symmetric matrix, then Q_2 generates a slender one, and Q_1 generates a flat one (see Fig.4). In this case, $\boldsymbol{m}_2$ accumulates near $\boldsymbol{n}_2$ and $\boldsymbol{m}_1$ accumulates near the $\boldsymbol{n}_1$-$\boldsymbol{n}_3$ plane. We pick the longest axis of Q_2 and the ellipse generated by two longer axes of Q_1 as a simple representation of two tensors, which reflects the major information.

Provided that $\boldsymbol{m}_2 = \boldsymbol{n}_2$, we examine the alignment of $\boldsymbol{m}_1$, which is confined to the plane $\boldsymbol{n}_1$-$\boldsymbol{n}_3$. Suppose $T = I$ and $s \geq 0$, which leads to $b_1 \geq 0$. The density function of $\boldsymbol{m}_1$ satisfies

$$f(\boldsymbol{m}_1) \propto \exp(b_1 m_{11} + b_{11} m_{11}^2).$$

Denote $K(m_{11}) = b_1 m_{11} + b_{11} m_{11}^2$. We describe three typical cases that cover the results we will present.

- Case I: $b_{11} < -b_1/2$. Typically when $|b_{11}|$ is very large, we have $q_{13} > q_{11}$. $K(m_{11})$ reaches its maximum at $m_{11}^{max} = -b_1/2b_{11} \in (0, 1)$. In this case, $\boldsymbol{m}_1$ accumulates at $m_{11} = m_{11}^{max}$, which two directions satisfy.
- Case II: $|b_{11}| < b_1/2$. Typically if b_1 is large, $|\boldsymbol{p}|$ is also large but q_{11} is not that large. In this case, $K(m_{11})$ is monotonely increasing in $[-1, 1]$. Thus $\boldsymbol{m}_1$ accumulates at $m_{11} = 1$.

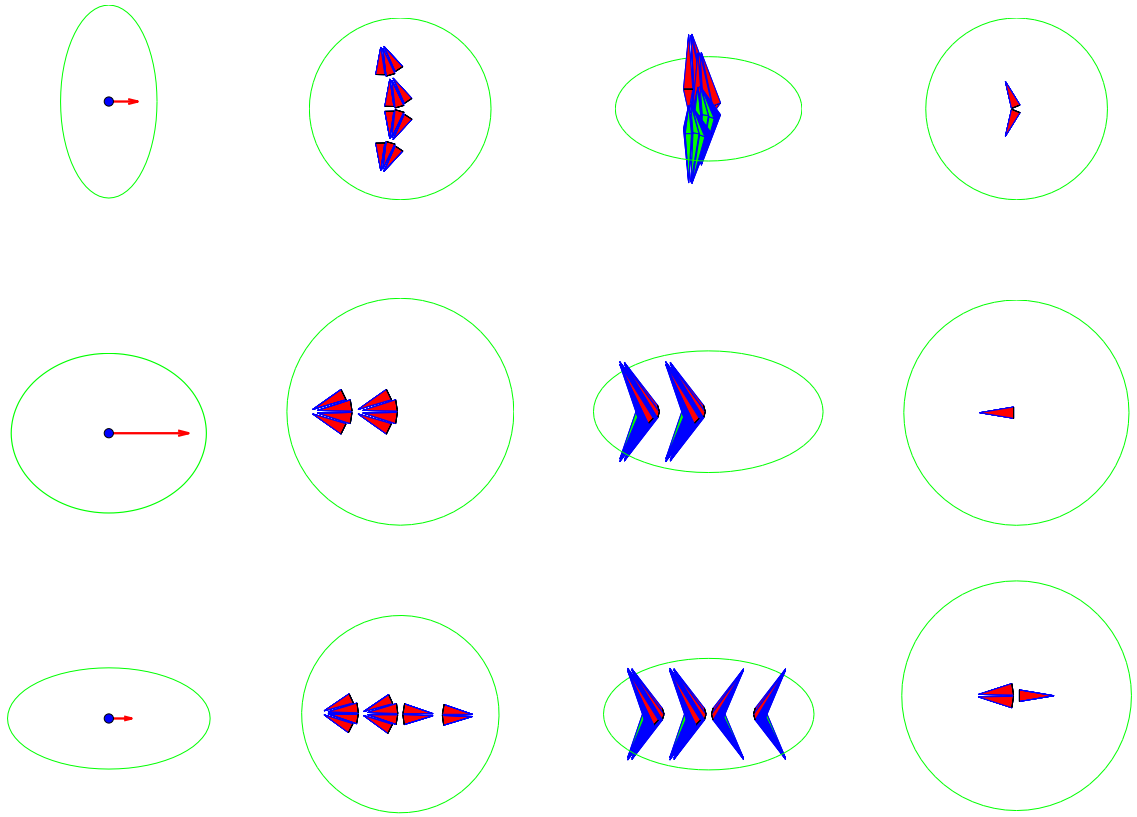

Figure 5: Three cases of alignment. From left to right in each row: the representation of Q_i (see Fig.4) and the plot of $\boldsymbol{p}$ (drawn in red); the alignment of molecules (viewed from $\boldsymbol{n}_2$); the alignment of molecules (oblique view); an abstract representation of the alignment (top view). Upper: $q_{13} > q_{11}$ with small s, corresponding to $b_{11} < -b_1/2$. The molecules align near two preferred orientations between $\mathrm{sgn}(s)\boldsymbol{n}_1$ and $\pm\boldsymbol{n}_3$. Middle: $s \gg 0$ with q_{11} not large, corresponding to $-b_1/2 < b_{11} < b_1/2$ with large b_1. The molecules prefer to align near $\mathrm{sgn}(s)\boldsymbol{n}_1$. Lower: $q_{13} \ll q_{11}$ with small s, corresponding to large $b_{11} > 0$ with small b_1. The molecules prefer to align near $\pm\boldsymbol{n}_1$, and more near $\mathrm{sgn}(s)\boldsymbol{n}_1$.

Figure 6: Schematic of the twist-bend phase (the right-handed case). The red and the blue line represents $\boldsymbol{n}_1$ and $\boldsymbol{n}_2$ respectively. $\boldsymbol{n}_1$ rotates on a circle, and $\boldsymbol{n}_2$ rotates on a circular cone.

- Case III: Large $b_{11} > 0$ with small b_1. In this case, q_{11} is large while $|\boldsymbol{p}|$ is small. Then $K(m_{11})$ reaches maximum at $m_{11} = 1$ and $K(-1)$ is a little smaller than $K(1)$. In this case, $\boldsymbol{m}_1$ accumulates at $m_{11} = \pm 1$ with a little more at $m_{11} = 1$.

The three cases are drawn in Fig.5. In the following, we will draw a molecule in each orientation where $K(m_{11})$ reaches maximum for case I, and will draw a molecule such that $\boldsymbol{m}_1 = \mathrm{sgn}(s)\boldsymbol{n}_1$ for case II. And for case III, we will draw a molecule for both $\boldsymbol{m}_1 = \pm\boldsymbol{n}_1$, and an extra one for $\boldsymbol{m}_1 = \mathrm{sgn}(s)\boldsymbol{n}_1$ if $\boldsymbol{p} \neq \boldsymbol{0}$.

When $c_{11} = c_{11}^{(0)}/2,\ c_{12} = c_{12}^{(0)}/1.2$, the model exhibits the twist-bend phase and the splay-bend phase. The twist-bend phase (N_{tb}) is featured by its helical modulation, with $T(x)$ written as

$$T(x) = \begin{pmatrix} 0 & -\cos\gamma_0 & \sin\gamma_0 \\ \cos\frac{2\pi x}{L} & -\sin\gamma_0 \sin\frac{2\pi x}{L} & -\cos\gamma_0 \sin\frac{2\pi x}{L} \\ \sin\frac{2\pi x}{L} & \sin\gamma_0 \cos\frac{2\pi x}{L} & \cos\gamma_0 \cos\frac{2\pi x}{L} \end{pmatrix}. \tag{3.2}$$

We know from this expression that $T(x)$ rotates at a constant speed round the x-axis with $\boldsymbol{p}$ keeping perpendicular to the x-axis. The axis $\pm\boldsymbol{n}_2$ forms a fixed angle γ_0 with the x-axis. The eigenvalues s and q_{ij} are constant in space with large $|s|$ and $s < 0$, corresponding to case II. If we pick the most probable orientation, the structure we obtain is equivalent to what is obtained in [10]. The variation of eigenframe is drawn in Fig.6.

In the above, $\boldsymbol{p}$ rotates on a right-handed helix. It may also rotate on a left-handed helix. Namely, leave s and q_{ij} unchanged and let

$$T(x) = \begin{pmatrix} 0 & \cos\gamma_0 & \sin\gamma_0 \\ \cos\frac{-2\pi x}{L} & -\sin\gamma_0 \sin\frac{-2\pi x}{L} & \cos\gamma_0 \sin\frac{-2\pi x}{L} \\ \sin\frac{-2\pi x}{L} & \sin\gamma_0 \cos\frac{-2\pi x}{L} & -\cos\gamma_0 \cos\frac{-2\pi x}{L} \end{pmatrix}, \tag{3.3}$$

we get the left-handed structure that is of the same energy as the right-handed structure. It is not surprising because of the achiral molecular structure.

In both right-handed and left-handed cases, the bending vector of $\boldsymbol{n}_2$ points along $\boldsymbol{n}_1$.

$$\boldsymbol{n}_2 \times (\nabla \times \boldsymbol{n}_2) = \frac{2\pi}{L}\cos\gamma_0 \sin\gamma_0 (0, \cos\frac{\pm 2\pi x}{L}, \sin\frac{\pm 2\pi x}{L})^T = \frac{2\pi}{L}\cos\gamma_0 \sin\gamma_0 \boldsymbol{n}_1.$$

It is worth noting that $s < 0$, which indicates that $\boldsymbol{p}$ points opposite to the bending vector. In fact, it origins from the sign of c_{12}, which will be discussed later.

Next we describe the splay-bend phase(N_{sb}). We plot q_{1i}, s and α in Fig.7. $T(x)$ is of the following form.

$$T(x) = \begin{pmatrix} \cos\alpha(x) & -\sin\alpha(x) & 0 \\ \sin\alpha(x) & \cos\alpha(x) & 0 \\ 0 & 0 & 1 \end{pmatrix}, \tag{3.4}$$

with $\alpha(x)$ oscillating near $\pi/2$. This implies that $\boldsymbol{n}_2$ swings near the x-axis in the x-y plane. $|s|$ reaches its maxima where $\alpha = \pi/2$, and zero where α is the farthest from $\pi/2$. Note that the difference between q_{11} and q_{13} is not large anywhere, and $q_{13} > q_{11}$ where $|s|$ is small. Therefore the alignment corresponds to case I near $x = 0, L/2$ and case II in between. The alignment is drawn in Fig.8 using the abstract representation in Fig.5.

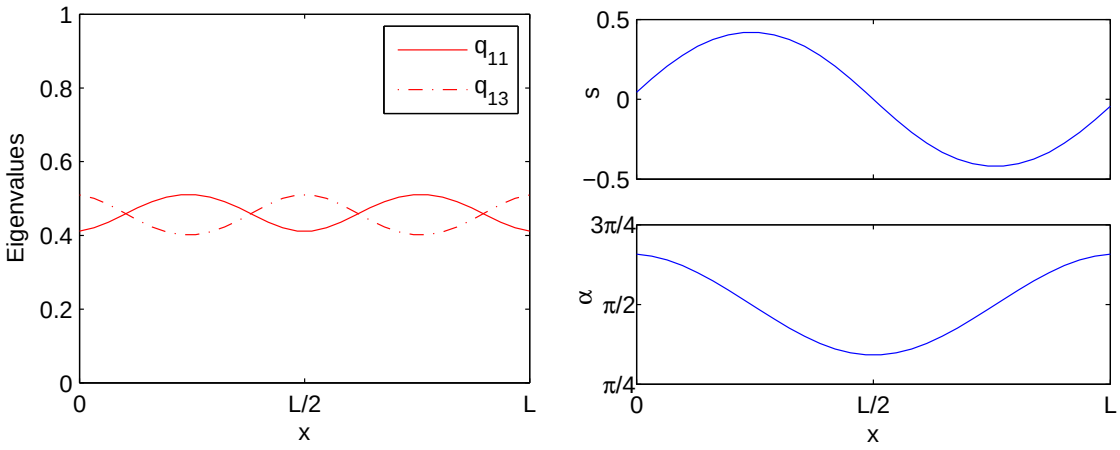

Figure 7: Eigenvalues and the Euler angle α of the splay-bend phase. The parameters are chosen as $c_{11} = c_{11}^{(0)}/2$, $c_{12} = c_{12}^{(0)}/1.2$ and $c = 15.0$. Left: eigenvalues of Q_1. Upper right: s. Lower right: α.

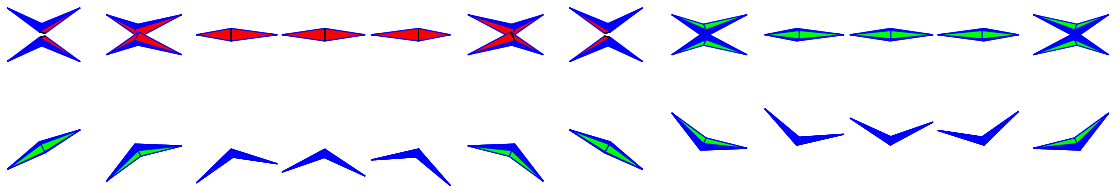

Figure 8: Schematic of the splay-bend phase. Upper: side view. Lower: top view.

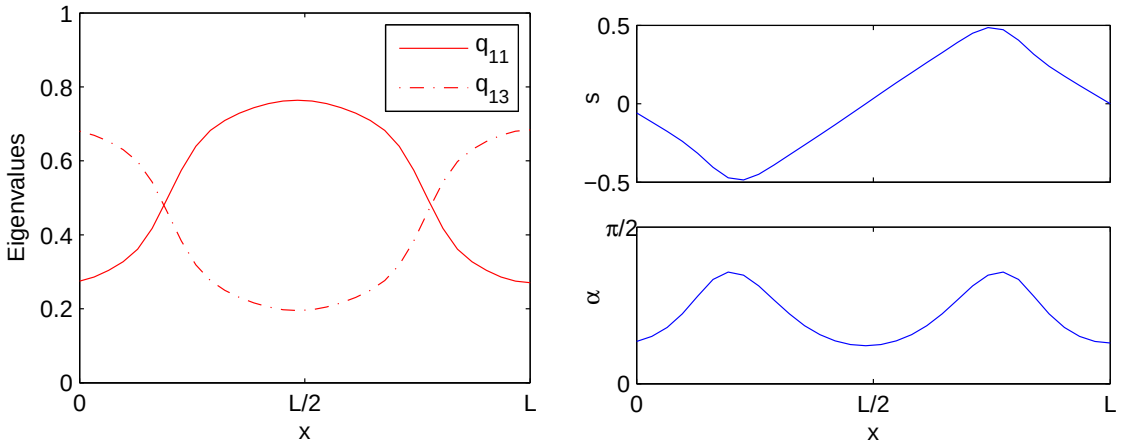

Figure 9: Eigenvalues and the Euler angle α of the swing phase. The parameters are chosen as $c_{11} = c_{11}^{(0)}/2$, $c_{12} = c_{12}^{(0)}/2$ and $c = 25.0$. Left: eigenvalues of Q_1. Upper right: s. Lower right: α.

Figure 10: Schematic of the swing phase. Side view.

Here we also calculate the bending vector of $\boldsymbol{n}_2$.

$$\boldsymbol{n}_2 \times (\nabla \times \boldsymbol{n}_2) = \frac{\mathrm{d}\alpha}{\mathrm{d}x} \sin\alpha (\cos\alpha, \sin\alpha, 0)^T = \frac{\mathrm{d}\alpha}{\mathrm{d}x} \sin\alpha \boldsymbol{n}_1.$$

Note that s and $\mathrm{d}\alpha/\mathrm{d}x$ always have the opposite sign, which indicates that $\boldsymbol{n}_1$ points opposite to the bending direction of $\boldsymbol{n}_2$.

When we shrink c_{12} to $c_{12}^{(0)}/2$, the twist-bend phase and the splay-bend phase become unstable. A stable phase distinct from the above two is found. In this phase $T(x)$ reads

$$T(x) = \begin{pmatrix} \cos\alpha(x) & 0 & \sin\alpha(x) \\ 0 & -1 & 0 \\ \sin\alpha(x) & 0 & -\cos\alpha(x) \end{pmatrix}, \tag{3.5}$$

where α oscillates in an interval that is contained in $(0, \pi/2)$, as is plotted in Fig.9. The axis $\boldsymbol{n}_2$ coincides with the y-axis. The $\boldsymbol{n}_1$-$\boldsymbol{n}_3$ plane shows a swinging pattern as α oscillates. We name it the swing phase (N_{sw}). In this phase, q_{11} and q_{13} dominate alternatively among the eigenvalues of Q_1. The largest $|s|$ occurs near where $q_{11} = q_{13}$, and $s \approx 0$ where $|q_{11} - q_{13}|$ is large. This suggests the following pattern of alignment: case I — case II — case III — case II — case I. It is drawn in Fig.10.

A metastable phase is found such that $T(x) = I$. We plot in Fig.11 the eigenvalues for $c_{11} = c_{11}^{(0)}/1.5$, $c_{12} = c_{12}^{(0)}/2$ and $c = 20.0$. By looking at the eigenvalues, we know that this phase has the same pattern of alignment as N_{sw} phase, but does not include the rotation of eigenframe. As the preferred orientation of $\boldsymbol{m}_1$ alters between x- and z-direction, we denote the phase as N_{alt}. The alignment is drawn in Fig.12.

The following phase sequences are found under various coefficients.

- $c_{11} = c_{11}^{(0)}/2,\ c_{12} = c_{12}^{(0)}/1.2.$

$$I \xrightarrow{c\approx 10.1} N_2 \xrightarrow{c\approx 11.0} N_{tb}.$$

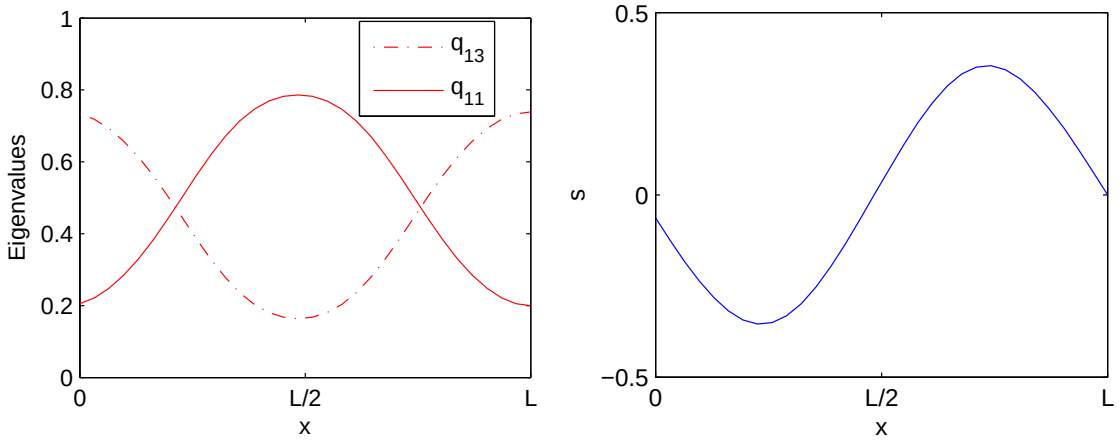

Figure 11: Eigenvalues of N_{alt} phase. The parameters are chosen as $c_{11} = c_{11}^{(0)}/1.5$, $c_{12} = c_{12}^{(0)}/2$ and $c = 20.0$. The local orthonormal frame is $T(x) = I$. Left: eigenvalues of Q_1. Right: s.

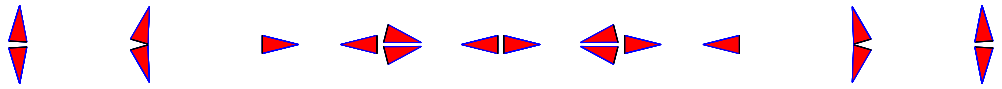

Figure 12: Schematic of N_{alt} phase. Side view.

- $c_{11} = c_{11}^{(0)}/2,\ c_{12} = c_{12}^{(0)}/0.6.$

$$I \xrightarrow{c\approx 4.3} N_{tb}.$$

- $c_{11} = c_{11}^{(0)}/2,\ c_{12} = c_{12}^{(0)}/2.$

$$I \xrightarrow{c\approx 10.1} N_2 \xrightarrow{c\approx 24.5} N_{sw}.$$

- $c_{11} = c_{11}^{(0)},\ c_{12} = c_{12}^{(0)}/2.$

$$I \xrightarrow{c\approx 9.3} N_{sw}.$$

It implies that with larger c_{12}, the direct I-N_{tb} sequence occurs; with smaller c_{12}, the N_{tb} phase vanishes; and the I-N-N_{tb} sequence occurs in between.

3.3 Discussion

In the experimental work by Borshch *et al.* [4], the phase sequence I-N-N_{tb} has been reported on cooling. In our model, the increase of c can be viewed analogous to the decrease of the temperature. Thus the first sequence we get is consistent with the experiments. To our knowledge, there is no preceding model that contains the complete I-N-N_{tb} sequence. The isotropic-helix transition has been observed for chiral molecule [23]. Our model shows the possibility for achiral molecule, which is interesting to see if it can be observed.

It is common in previous works to utilize an axis and a polarizationto describe the local orientation. In our model and the choice of coefficients, we may view $\boldsymbol{n}_2$ and $\boldsymbol{p}$ as the axis and the polarization. If we look only at $\boldsymbol{n}_2$ and $\boldsymbol{p}$, the twist-bend and the splay-bend structures are the same as those obtained in [10]. And the presence of Q_1 provides information more detailed on molecular alignment for the splay-bend phase where $\boldsymbol{p} \approx \boldsymbol{0}$. Moreover, it is able to generate N_{sw} phase and N_{alt} phase that are not included previously, where the $\boldsymbol{n}_2$ is spatially invariant. A criterion for the stabilization

of the splay-bend phase has been proposed in [3] and [10], but we have not found the coefficients that stabilize the splay-bend phase, which needs a thorough examination in the future.

Another interesting topic is about the direction of $\boldsymbol{p}$. Note that the change of $\boldsymbol{p}$ to $-\boldsymbol{p}$ does not affect the bulk and the second elastic energy.

$$F_{bulk}[\boldsymbol{p}, Q_1, Q_2] = F_{bulk}[-\boldsymbol{p}, Q_1, Q_2],$$
$$F^{(2)}_{elastic}[\boldsymbol{p}, Q_1, Q_2] = F^{(2)}_{elastic}[-\boldsymbol{p}, Q_1, Q_2].$$

Therefore, whether $\boldsymbol{p}$ or $-\boldsymbol{p}$ is favoured is determined by $F^{(1)}_{elastic}$. Under certain circumstances, the signs of c_{11} and c_{12} imply the preference among $\boldsymbol{p}$ and $-\boldsymbol{p}$. In fact, the first elastic energy can be written as

$$\begin{aligned} F^{(1)}_{elastic} = \int \mathrm{d}\boldsymbol{x} \Big[&(\boldsymbol{p}\cdot\nabla)(c_{11}q_{11} + c_{12}q_{21}) + \big(c_{11}(q_{12}-q_{11}) + c_{12}(q_{22}-q_{21})\big)\boldsymbol{p}\cdot\boldsymbol{n}_2 \times (\nabla\times\boldsymbol{n}_2) \\ &+ \big(c_{11}(q_{13}-q_{11}) + c_{12}(q_{23}-q_{21})\big)\boldsymbol{p}\cdot\boldsymbol{n}_3 \times (\nabla\times\boldsymbol{n}_3)\Big]. \end{aligned}$$

In the twist-bend phase where s, q_{ij} are constants, using

$$\begin{aligned} \boldsymbol{n}_1\cdot\boldsymbol{n}_2\times(\nabla\times\boldsymbol{n}_2) =& -n_{1i}n_{2j}\partial_j n_{2i} \\ =& n_{2i}n_{2j}\partial_j n_{1i} \\ =& (I - n_{1i}n_{1j} - n_{3i}n_{3j})\partial_j n_{1i} \\ =& \nabla\cdot\boldsymbol{n}_1 - \boldsymbol{n}_1\cdot\boldsymbol{n}_3\times(\nabla\times\boldsymbol{n}_3), \end{aligned}$$

$F^{(1)}_{elastic}$ is simplified to

$$F^{(1)}_{elastic} = \big(c_{11}(q_{12}-q_{13}) + c_{12}(q_{22}-q_{23})\big)\int \mathrm{d}\boldsymbol{x}\boldsymbol{p}\cdot\boldsymbol{n}_2\times(\nabla\times\boldsymbol{n}_2).$$

In the first parenthesis, $c_{12}q_{22}$ dominates, thus determines the sign. Because it is positive, we know that $\boldsymbol{p}$ tends opposite to the bending vector of $\boldsymbol{n}_2$.

In the splay-bend phase, $\boldsymbol{n}_3$ is constant. In the second term in $F^{(1)}_{elastic}$, the dominant coefficient is $c_{12}q_{22} > 0$. Therefore $\boldsymbol{p}$ tends to be opposite to the bending vector of $\boldsymbol{n}_2$. In the first term, $\nabla(c_{11}q_{11})$ dominates as q_{21} fluctuates little, indicating that the x-component of $\boldsymbol{p}$ tends to have opposite sign of $\mathrm{d}q_{11}\mathrm{d}x$. This is consistent with the tendency generated by the second term.

In [10] where the coupling of polarization and the bending vector is modelled explicitly, the polarization is assumed to prefer along the bending. It is proposed without any evidence. Our estimation, which is deduced from molecular theory, is contrary to this assumption.

At last, in the N_{alt} phase, the sign of c_{11} implies that $\boldsymbol{p}$ tends to point to the position where $\boldsymbol{m}_1$ aligns along the z-axis. Now only the first term occurs. Again the dominant term is $\nabla(c_{11}q_{11})$, which implies that $\boldsymbol{p}$ prefers along the decreasing direction of q_{11}.

4 Conclusion

A tensor model for bent-core molecules is constructed. Its form, as well as its coefficients, is derived from the molecular theory. Besides the homogeneous nematic phases, the twist-bend phase and the splay-bend phase can be captured, along with two new phases. In the future, the model is expected to be investigated systematically, no matter for phase behaviors and for surface-induced phenomena. The method to determine the coefficients is also worth further discussion. Moreover, we are looking to extend the model to smectic and columnar phases.

5 Appendix

5.1 The properties of the closure

Let

$$\mathcal{A} = \{(s, q_{ij}) | \rho : SO_3 \to \mathbb{R}^+,\ \int \mathrm{d}\nu\rho = 1,\ s = \int \mathrm{d}\nu\rho m_{11},\ q_{ij} = \int \mathrm{d}\nu\rho m_{ij}^2,\ i,j = 1,2.\}.$$

Theorem 5.1. *Each $(s, q_{ij}) \in \mathcal{A}$ is subject to the constraints in (2.11). For any $(s, q_{ij}) \in \mathcal{A}$, there exists a unique solution to the minimization problem*

$$\begin{aligned}
&\inf \int_{SO_3} \mathrm{d}\nu\rho(P)\log\rho(P),\\
s.t.\ &\int \mathrm{d}\nu\rho(P) = 1,\\
&\int \mathrm{d}\nu \boldsymbol{m}_1\rho(P) = (s,0,0)^T,\\
&\int \mathrm{d}\nu \boldsymbol{m}_1\boldsymbol{m}_1\rho(P) = diag(q_{11}, q_{12}, 1-q_{11}-q_{12}),\\
&\int \mathrm{d}\nu \boldsymbol{m}_2\boldsymbol{m}_2\rho(P) = diag(q_{21}, q_{22}, 1-q_{21}-q_{22}).
\end{aligned}$$

The solution takes the form

$$\rho(P) = \frac{1}{Z}\exp\left(b_1 m_{11} + \sum_{i,j=1,2} b_{ij} m_{ij}^2\right),$$

where

$$Z = \int \mathrm{d}\nu \exp\left(b_1 m_{11} + \sum_{i,j=1,2} b_{ij} m_{ij}^2\right).$$

Therefore, $\mathcal{A} = \{(s, q_{ij}) : (s, q_{ij})$ satisfies (2.11).$\}$.

Proof. Note that

$$\begin{aligned}
m_{13}^2 &= 1 - m_{11}^2 - m_{12}^2 \geq 0,\\
m_{23}^2 &= 1 - m_{21}^2 - m_{22}^2 \geq 0,\\
m_{31}^2 &= 1 - m_{11}^2 - m_{21}^2 \geq 0,\\
m_{32}^2 &= 1 - m_{12}^2 - m_{22}^2 \geq 0,\\
m_{33}^2 &= m_{11}^2 + m_{12}^2 + m_{11}^2 + m_{12}^2 - 1 \geq 0,
\end{aligned}$$

and that for $i,j = 1,2,3$, the measure of the set $\{P : m_{ij} = 0\}$ is zero. Thus the first six inequalities in (2.11) are obtained. The last inequality in (2.11) comes from $(\int \mathrm{d}\nu f m_{11})^2 \leq \int \mathrm{d}\nu f m_{11}^2$, and that the equality holds only if $f m_{11} = \lambda f$ holds for a constant λ, which implies that $f = 0$ for $m_{11} \neq \lambda$. Again we note that the measure of the set $\{P : m_{11} = \lambda\}$ is zero.

The uniqueness of f is deduced immediately from the strict convexity of $f\log f$ about f.

To prove the existence, consider the function

$$J(b_1, b_{ij}) = \int \mathrm{d}\nu \exp\left(b_1(m_{11} - s) + \sum_{i,j=1,2} b_{ij}(m_{ij}^2 - q_{ij})\right). \tag{5.1}$$

A stationary point of J satisfies $\partial J/\partial b_1 = \partial J/\partial b_{ij} = 0$, which yields

$$s = \frac{1}{Z}\int \mathrm{d}\nu \exp\left(b_1 m_{11} + \sum_{i,j=1,2} b_{ij} m_{ij}^2\right) m_{11},$$
$$q_{ij} = \frac{1}{Z}\int \mathrm{d}\nu \exp\left(b_1 m_{11} + \sum_{i,j=1,2} b_{ij} m_{ij}^2\right) m_{ij}^2, \quad i,j = 1,2.$$

From the Euler-Lagrange equation (2.10) and the uniqueness, the stationary point of J solves the minimization problem. We will prove that

$$\lim_{b_1^2+\sum b_{ij}^2 \to \infty} J = +\infty. \tag{5.2}$$

Since J is bounded from below, (5.2) indicates the existence of a minimum.

For (5.2), it is sufficient to prove that for any

$$(b_1, b_{11}, b_{12}, b_{21}, b_{22}) \neq (0,0,0,0,0),$$

there exists a P such that

$$I(P) = b_1(m_{11} - s) + \sum_{i,j=1,2} b_{ij}(m_{ij}^2 - q_{ij}) > 0.$$

Let

$$P_1 = \begin{pmatrix} 1 & 0 & 0 \\ 0 & 0 & 1 \\ 0 & -1 & 0 \end{pmatrix}, \quad P_2 = \begin{pmatrix} -1 & 0 & 0 \\ 0 & 0 & 1 \\ 0 & 1 & 0 \end{pmatrix}, \quad P_3 = \begin{pmatrix} 1 & 0 & 0 \\ 0 & 1 & 0 \\ 0 & 0 & 1 \end{pmatrix}, \quad P_4 = \begin{pmatrix} -1 & 0 & 0 \\ 0 & 1 & 0 \\ 0 & 0 & -1 \end{pmatrix},$$
$$P_5 = \begin{pmatrix} 0 & 1 & 0 \\ 0 & 0 & 1 \\ 1 & 0 & 0 \end{pmatrix}, \quad P_6 = \begin{pmatrix} 0 & 0 & 1 \\ 1 & 0 & 0 \\ 0 & 1 & 0 \end{pmatrix}, \quad P_7 = \begin{pmatrix} 0 & 0 & -1 \\ 0 & 1 & 0 \\ 1 & 0 & 0 \end{pmatrix}, \quad P_8 = \begin{pmatrix} 0 & 1 & 0 \\ 1 & 0 & 0 \\ 0 & 0 & -1 \end{pmatrix}.$$

It is straightforward to verify that

$$\lambda_i I(P_i) = 0$$

holds for arbitrary (b_1, b_{ij}) where

$$\begin{aligned}
\lambda_1 &= (\lambda - q_{22})\left(\frac{1}{2} + \frac{s}{2q_{11}}\right), \\
\lambda_2 &= (\lambda - q_{22})\left(\frac{1}{2} - \frac{s}{2q_{11}}\right), \\
\lambda_3 &= (q_{11} + q_{22} - \lambda)\left(\frac{1}{2} + \frac{s}{2q_{11}}\right), \\
\lambda_4 &= (q_{11} + q_{22} - \lambda)\left(\frac{1}{2} - \frac{s}{2q_{11}}\right), \\
\lambda_5 &= 1 - \lambda - q_{12}, \\
\lambda_6 &= 1 - \lambda - q_{21}, \\
\lambda_7 &= \lambda - q_{11}, \\
\lambda_8 &= q_{12} + q_{21} - (1 - \lambda).
\end{aligned}$$

Here λ is a real number to be determined. We choose a λ such that $\lambda_i > 0$. It is equivalent to

$$\begin{aligned}
\lambda - q_{22} &> 0,\\
q_{11} + q_{22} - \lambda &> 0,\\
\lambda - q_{11} &> 0,\\
1 - \lambda - q_{12} &> 0,\\
1 - \lambda - q_{21} &> 0,\\
q_{21} + q_{12} - (1 - \lambda) &> 0,
\end{aligned}$$

which yields

$$\max\{q_{11}, q_{22}, 1 - q_{12} - q_{21}\} < \lambda < \min\{1 - q_{12}, 1 - q_{21}, q_{11} + q_{22}\}.$$

From the constraints on q_{ij}, the upper bound is greater than the lower bound, which guarantees the existence of λ. Note that

$$\sum_{i=1}^{8} \lambda_i = 1.$$

Let

$$A = b_1 s + \sum_{i,j=1,2} b_{ij} q_{ij}.$$

We claim that $I(P_i) > 0$ for some i. Otherwise $I(P_i) = 0$ for every i. Expanding these equalities, we have

$$\begin{aligned}
\pm b_1 + b_{11} &= A,\\
\pm b_1 + b_{11} + b_{22} &= A,\\
b_{21} &= A,\\
b_{12} &= A,\\
b_{22} &= A,\\
b_{12} + b_{21} &= A.
\end{aligned}$$

It is easy to deduce that $b_1 = b_{ij} = 0$. □

5.2 The computation of (2.5) for bent-core molecules from hardcore potential

Denote by T_0 the broken line of a molecule (see Fig.2) posed such that two eigenframes $(\hat{O}; \boldsymbol{m}_i)$ and $(O; \boldsymbol{e}_i)$ coincide. Let $T_1 = PT_0$ and $T_2 = P'T_0$. When using the hardcore potential, $G(\boldsymbol{r}, P, P')$ takes one if two molecules touch and zero if not. The condition for $G(\boldsymbol{r}, P, P') = 1$ can be written as

$$\boldsymbol{r} \in T_1 - T_2 + B_D,$$

where B_D denotes a sphere of radius D. Here $A \pm B$ represents

$$A \pm B = \{a \pm b | a \in A, b \in B\}.$$

This is because the region occupied by two molecules are $T_1 + \boldsymbol{x} + B_{D/2}$ and $T_2 + \boldsymbol{x'} + B_{D/2}$ respectively.

Denote by $\boldsymbol{p}_1$ and $\boldsymbol{p}_2$ the vectors pointing from the arrowhead to two ends of the broken line T_1, namely two 'arms' of T_1, and by $\boldsymbol{p}'_1$ and $\boldsymbol{p}'_2$ two arms of $-T_2$. Then

$$\begin{aligned}
T_1 - T_2 + B_D &= \Big(\{O\boldsymbol{p}_1\} \cup \{O\boldsymbol{p}_2\}\Big) + \Big(\{O\boldsymbol{p}'_1\} \cup \{O\boldsymbol{p}'_2\}\Big) + B_D\\
&= \bigcup_{i,j=1,2} \Big(O\boldsymbol{p}_i\boldsymbol{p}'_j + B_D\Big),
\end{aligned}$$

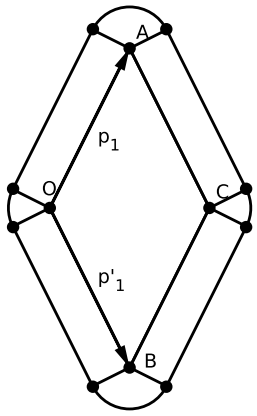

Figure 13: Intersection of a spheroparallelogram and the plane $z = 0$.

which is the union of four spheroparallelograms (the sum of a sphere and a parallelogram),

$$V_{ij} = O\boldsymbol{p}_i\boldsymbol{p}'_j + B_D, \qquad i, j = 1, 2.$$

Note that V_{ij} are convex that share O, which indicates that if $R \in V$, then $\lambda R \in V$ for $0 \le \lambda \le 1$. Denote

$$r_{ij}(\boldsymbol{n}) = \max_{s\boldsymbol{n}\in V_{ij}} s$$

and

$$r(\boldsymbol{n}) = \max_{i,j=1,2} r_{ij}(\boldsymbol{n}).$$

We can express $M^{(k)}$ by an integral in spherical coordinates.

$$\begin{aligned} M^{(k)}(P, P') &= \int_{T_1-T_2+B_D} \underbrace{\boldsymbol{r}\dots\boldsymbol{r}}_{k \text{ times}} \,\mathrm{d}\boldsymbol{r} \\ &= \int_{S^2} \underbrace{\boldsymbol{n}\dots\boldsymbol{n}}_{k \text{ times}} \,\mathrm{d}\boldsymbol{n} \int_0^{r(\boldsymbol{n})} \mathrm{d}r r^{k+2} \\ &= \int_{S^2} \frac{1}{k+3} r(\boldsymbol{n})^{k+3} \underbrace{\boldsymbol{n}\dots\boldsymbol{n}}_{k \text{ times}} \,\mathrm{d}\boldsymbol{n}. \end{aligned}$$

Now we need to give an expression of r_{ij}. We may place the parallelogram $O\boldsymbol{p}_i\boldsymbol{p}'_j$ in the plane $z = 0$. Denote by R the intersection point of the ray $s\boldsymbol{n}$ and the spheroparallelogram. We need to determine where R lies. We follow the procedure below.

- Compute the intersection point of the ray $s\boldsymbol{n}$ and the plane $z = D$. Then examine whether its projection on the plane $z = 0$ lies in the parallelogram $OACB$, plotted in Fig.13. If yes, the R lies on the flat surface of the spheroparallelogram.
- Determine whether the ray $s\boldsymbol{n}$ intersects with any of the spheres on the corner. If yes, compute the farthest intersection point and examine its projection on the plane $z = 0$. If it lies in the corresponding sector (located at the corners in Fig.13), R lies on the spherical surface of the spheroparallelogram.
- Now we know that R lies on the cylindrical surface of the spheroparallelogram, and it is easy to distinguish which cylinder it locates.

Acknowledgments. P. Zhang is partially supported by National Natural Science Foundation of China (Grant No. 50930003, 21274005, and 11421110001).

References

[1] D. A. Coleman, J. Fernsler, N. Chattham, M. Nataka, Y. Takanishi, E. Körblova, D. R. Link, R.-F. Shao, W. G. Jang, J. E. Maclennan, O. Mondainn-Monval, C. Boyer, W. Weissflog, G. Pelzl, L.-C Chien, J. Zasadzinski, J. Watanabe, D. M. Walba, H. Takezoe, and N. A. Clark. *Science*, 301:1204, 2003.

[2] H. Takezoe and Y. Takanishi. *Jpn. J. Appl. Phys.*, 45:597, 2006.

[3] I. Dozov. *Europhys. Lett.*, 56:247, 2001.

[4] V. Borshch, Y.-K. Kim, J. Xiang, M. Gao, A. Jákli, V. P. Panov, J. K. Vij, C. T. Imrie, M. G. Tamba, G. H. Mehl, and O. D. Lavrentovich. *Nat. Commun.*, 4:2635, 2013.

[5] D. Chen, J. H. Porada, J. B. Hooper, A. Klittnick, Y. Shen, M. R. Tuchband, E. Korblova, D. Bedrov, D. M. Walba, M. A. Glaser, J. E. Maclennan, and N. A. Clark. *Proc. Natl. Acad. Sci. USA*, 110:15931, 2013.

[6] V. L. Lorman and B. Mettout. *Phys. Rev. Lett.*, 82:940, 1999.

[7] A. Roya and N. V. Madhusudana. *Europhys. Lett. J. E*, 18:253, 2005.

[8] A. Roy, N. V. Madhusudana, P. Tolédano, and A. M. Figueiredo Neto. *Phys. Rev. Lett.*, 82:1466, 1999.

[9] N. Vaupotič, M. Čopič, E. Gorecka, and D. Pociecha. *Phys. Rev. Lett.*, 98:247802, 2007.

[10] S. M. Shamid, S. Dhakal and J. V. Selinger. *Phys. Rev. E*, 87:052503, 2013.

[11] N. Vaupotič, M. Čepič, M. A. Osipov, and E. Gorecka. *Phys. Rev. E*, 89:030501, 2014.

[12] E. G. Virga. *Phys. Rev. E*, 89:052502, 2014.

[13] T. C. Lubensky and L. Radzihovsky. *Phys. Rev. E*, 66:031704, 2002.

[14] G. De Matteis, A. M. Sonnet and E. G. Virga. *Continuum. Mech. Thermodyn.*, 20:347, 2008.

[15] J. Xu and P. Zhang. *Sci. China. Math.*, 57:443, 2014.

[16] J. Han, Y. Luo, W. Wang and P. Zhang. *arXiv*, page 1305.4889, 2013.

[17] S. Mei and P. Zhang. *preprint.*

[18] P. G. De Genne. *Mol. Cryst. Liq. Cryst.*, 12:193, 1971.

[19] P. Sheng. *Phys. Rev. A*, 26:1610, 1982.

[20] J. I. Fukuda, M. Yoneya and H. Yokoyama. *Phys. Rev. E*, 65:041709, 2002.

[21] G. De Matteis and E. G. Virga. *Phys. Rev. E*, 71:061703, 2005.

[22] F. Bisi, E. G. Virga, E. C. Gartland, G. De Matteis, A. M. Sonnet, and G. E. Durand. *Phys. Rev. E*, 73:051709, 2006.

[23] A. Zep, S. Aya, K. Aihara, K. Ema, D. Pociecha, K. Madrak, P. Bernatowicz, H. Takezoe, and E. Gorecka. *J. Mater. Chem. C*, 1:46, 2013.